Journal of Engineering and Applied Sciences 3 (3): 271-278, 2008
ISSN: 1816-949X

Numerical Investigation of Natural Turbulent Convection in a Square Cavity

K. Bouaraour
Laboratoire d'Energétique Appliqué et de Pollution, Département de Génie Mécanique,
Université Mentouri, Route de Ain El Bey 25000 Constantine, Algérie

Abstract: In this study, we are interesting to the numeric al simulation of the turbulent natural convection in a square cavity, with differentially heated vertical walls and with adiabatic horizontal ones. The selected problem has been broadly studied due to many applications in engineering, such as solar collectors, conservation of energy in buildings and cooling electronic devices. Turbulence is modelled by the low Reynolds number k-ε model of Launder (1974). The equations controlling the flow are discretized using the finite volumes method. The SIMPLER algorithm is used for the Pressure-Velocity coupling and the sweeping method with the algorithm of Thomas (TDMA) is used for the iterative solution of the systems of the equations. For the 2 selected Rayleigh numbers: $Ra=1.58*10^9$ and $Ra=4.9*10^{10}$, the numerical results obtained concerning the dynamic field, the thermal field and the various turbulent quantities, show a good agreement with the experimental results of Tian and with the numerical results of Sharif and those of Hsieh.

Key words: Natural turbulent convection, k-ε model, finite volumes

INTRODUCTION

Natural convection in rectangular cavities is a subject of investigation of great importance because of its fundamental importance and its presence in different industrial applications including electronic cooling, losses of heat in solar heat collectors and ventilation of constructions.

Most of the early studies were focused on laminar flows and on the stages of its transition to turbulence, where it achieved considerable success. However, turbulent flows which is the mode of flow generally met in nature is still a challenge both in experimental and in numerical terms, especially when low level of turbulence exists. In addition to the experimental research of Cheesewright *et al.* (1986), reported by Davidson (1990) for cavities with aspect ratio equal to 5, recently we found those of Tian and Karayiannis (2000) and those of Bett and Bokhari (2000), for cavities with aspect ratios equal, respectively to 1 and 28.68. These examples are often used to validate natural turbulence convection models in cavities.

For important variations in temperatures, which correspond to sufficiently high Rayleigh numbers, the flow close to the active walls is similar to the turbulent flow over a vertical flat plate, where there is formation of thermal and dynamic turbulent boundary layers. The

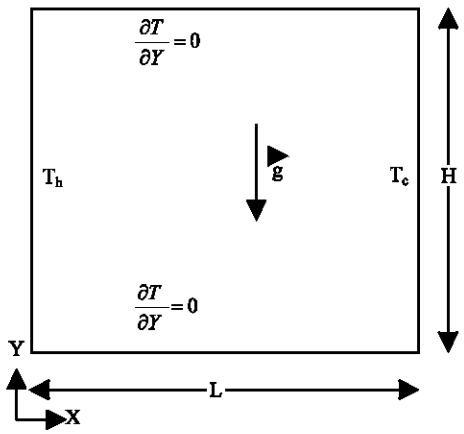

Fig. 1: Geometrical configuration and the coordinate system

standard k-ε model Launder (1974) was widely employed and has yielded reasonable solutions. However, numerical results obtained are not always in perfect agreement with the experimental data, especially near the walls in a stratified flow field. So, it would be very useful and practical to use a LRN k-ε turbulence model (Low Reynolds Number) to achieve stable and accurate solutions in numerical simulation. One of these models most often used is the model of Launder (1974), which tested its effectiveness for the rectangular cavities

configurations, as for other configurations (Tanaka, 1987; Henkes and Hoogendoorn, 1989). In this research, we studied numerically the turbulent natural convection inside a square cavity filled with air, where the horizontal walls are insulated and the vertical walls are kept up to uniform and different temperatures. Despite simplicity in geometry and boundary conditions, numerical predictions with various models showed significant discrepancies between each other and with the experimental data. The problem considered is depicted schematically in Fig. 1.

MATERIALS AND METHODS

Natural turbulent convection inside the cavity is modelled mathematically by the unsteady Reynolds average Navier-Stockes (RANS) equations expressing the conservation of mass, momentum and energy. The following assumptions are made:

- The Boussinesq approximation, which means that the variation of density is only important in the body force term of the governing equations.
- An incompressible fluid flow with negligible viscous dissipation.
- Constant fluid properties with no temperature dependence.
- No internal heat sources.

The resulting 2-dimensional system of partial differential equations in their dimensional form is represented below in a cartesian coordinate system (X,Y):

Conservation of mass:

$$\frac{\partial U}{\partial X}+\frac{\partial V}{\partial Y}=0 \tag{1}$$

X Momentum equation:

$$\frac{\partial U}{\partial t}+\frac{\partial}{\partial X}(U.U)+\frac{\partial}{\partial Y}(V.U)=-\frac{1}{\rho_0}\frac{\partial P}{\partial X}+\left[\frac{\partial}{\partial X}(\frac{\partial U}{\partial X})+\frac{\partial}{\partial Y}(\frac{\partial U}{\partial Y})\right]+\frac{\partial}{\partial X}\left[2\nu_t\left(\frac{\partial U}{\partial X}\right)-\frac{2}{3}K\right]+\frac{\partial}{\partial Y}\left[\nu_t\left(\frac{\partial U}{\partial Y}+\frac{\partial V}{\partial X}\right)\right] \tag{2}$$

Y Momentum equation:

$$\frac{\partial V}{\partial t}+\frac{\partial}{\partial X}(U.V)+\frac{\partial}{\partial Y}(V.V)=-\frac{1}{\rho_0}\frac{\partial P}{\partial Y}+\left[\frac{\partial}{\partial X}(\frac{\partial V}{\partial X})+\frac{\partial}{\partial Y}(\frac{\partial V}{\partial Y})\right]+\frac{\partial}{\partial X}\left[\nu_t\left(\frac{\partial U}{\partial Y}+\frac{\partial V}{\partial X}\right)\right]+\frac{\partial}{\partial Y}\left[2\nu_t\left(\frac{\partial V}{\partial Y}\right)-\frac{2}{3}K\right]+g\beta(T-T_0) \tag{3}$$

Energy equation:

$$\frac{\partial T}{\partial t}+\frac{\partial}{\partial X}(U.T)+\frac{\partial}{\partial Y}(V.T)=\frac{\partial}{\partial X}\left[(\frac{\nu}{Pr}+\frac{\nu_t}{\sigma_t})\frac{\partial T}{\partial X}\right]+\frac{\partial}{\partial Y}\left[(\frac{\nu}{Pr}+\frac{\nu_t}{\sigma_t})\frac{\partial T}{\partial Y}\right] \tag{4}$$

U, V, P and T are, respectively the mean horizontal velocity, the mean vertical velocity, the mean dynamic pressure and the mean temperature.

g: Represents the gravitational acceleration in the vertical direction. ρ_0, V, V_t and β are the density at the reference temperature T_0 ($T_0 = T_c$), the molecular kinematic viscosity, the turbulent kinematic viscosity and the coefficient of thermal expansion.

$Pr = \nu/\alpha$ and σ_t are the Prandtl number and the turbulent Prandtl number, respectively, where α is the thermal diffusivity.

In order to account for the near wall effects, the turbulence model employed in this study is the LRN k-ε model of Jones and Launder, which gives accurate predictions for intermediate Reynolds numbers and for boundary layers. Its equations expressing the turbulent kinetic energy K and its function of dissipation ϵ, takes, respectively the following form:

$$\frac{\partial K}{\partial t}+\frac{\partial}{\partial X}(U.K)+\frac{\partial}{\partial Y}(V.K)=\frac{\partial}{\partial X}\left[(\nu+\frac{\nu_t}{\sigma_k})\frac{\partial K}{\partial X}\right]+\frac{\partial}{\partial Y}\left[(\nu+\frac{\nu_t}{\sigma_k})\frac{\partial K}{\partial Y}\right]+2\nu_t\left[\left(\frac{\partial U}{\partial X}\right)^2+\left(\frac{\partial V}{\partial Y}\right)^2\right]+\nu_t\left(\frac{\partial V}{\partial X}+\frac{\partial U}{\partial Y}\right)^2-\varepsilon-D \tag{5}$$

$$\frac{\partial \varepsilon}{\partial t}+\frac{\partial}{\partial X}(U.\varepsilon)+\frac{\partial}{\partial Y}(V.\varepsilon)=\frac{\partial}{\partial X}(\nu+\frac{\nu_t}{\sigma_\varepsilon})\frac{\partial \varepsilon}{\partial X}+$$
$$S\frac{\partial}{\partial Y}(\nu+\frac{\nu_t}{\sigma_\varepsilon})\frac{\partial \varepsilon}{\partial Y}+2\nu_t C_1 f_1\frac{\varepsilon}{K}\left[\left(\frac{\partial U}{\partial X}\right)^2+\left(\frac{\partial V}{\partial Y}\right)^2\right] \quad (6)$$
$$+\nu_t C_1 f_1\frac{\varepsilon}{K}\left(\frac{\partial V}{\partial X}+\frac{\partial U}{\partial Y}\right)^2-C_2 f_2\frac{\varepsilon^2}{K}+E$$

Like other LRN k-ε models of turbulence, this model is characterized by the additional term (D) in the turbulent kinetic energy equation and another term (E) in the dissipation equation. The expressions of these 2 terms are:

$$D=2\nu\left[\left(\frac{\partial\sqrt{K}}{\partial X}\right)^2+\left(\frac{\partial\sqrt{K}}{\partial Y}\right)^2\right] \quad (7)$$

$$E=2\nu\nu_t\left[\left(\frac{\partial^2 U}{\partial Y^2}\right)^2+\left(\frac{\partial^2 V}{\partial X^2}\right)^2\right] \quad (8)$$

The production terms due to the buoyancy is not included in this study, because it was found that buoyancy force is insignificant as a direct source of turbulence generation within the κ-ϵ model framework (Markatos *et al*., 1982), either when it is modelled by the isotropic SGD (Simple Gradient Diffusion) model or when it is modelled by the GGD (Generalized Gradient Diffusion) model.

Turbulent viscosity is connected to the turbulent kinetic energy and its function of dissipation by the Prandtl-Kolmogorov relation:

$$\nu_t=C_\mu f_\mu\frac{K^2}{\varepsilon} \quad (9)$$

$$f_\mu=\exp\left[\frac{-2.5}{\left(1+\frac{R_{et}}{50}\right)}\right] \quad (10)$$

$$f_1=1 \quad (11)$$

$$f_2=1-0.3\exp(-R_{et}^2) \quad (12)$$

The local turbulent Reynolds number is defined as follows:

$$R_{et}=\frac{K^2}{\nu\varepsilon} \quad (13)$$

The other constants of this model are:

$$C_\mu=0.09,\ \sigma_t=1,\ \sigma_K=1,\ \sigma_\varepsilon=1.3,\ C_1=1.44,\ C_2=1.92 \quad (14)$$

Other extra terms like the Yap correction proposed by Yap (1987) and reported by Ince and Launder (1974) can be added to the dissipation equation, but it found by Henkes and Hoogendoorn (1995) that the average Nusselt number is much better represented by the model without the inclusion of this correction in the ϵ equation.

For the resolution of the equations governing the studied phenomenon, we adopted the following initial conditions in the entire field:

$$\text{At } t=0: U=V=0, T=T_c, K=10^{-3}, \varepsilon=10^{-3} \quad (15)$$

For the boundary conditions at t>0:

$$X=0:\ U=V=0,\ T=T_h,\ K=0,\ \varepsilon=2\left(\frac{\partial\sqrt{K}}{\partial X}\right)^2\quad 0\le Y\le L$$

$$X=L:\ U=V=0,\ T=T_c,\ K=0,\ \varepsilon=2\left(\frac{\partial\sqrt{K}}{\partial X}\right)^2\quad 0\le Y\le L \quad (16)$$

$$Y=0:\ U=V=0,\ \frac{\partial T}{\partial Y}=0,\ K=0,\ \varepsilon=2\left(\frac{\partial\sqrt{K}}{\partial Y}\right)^2\quad 0\le X\le L$$

$$Y=L:\ U=V=0,\ \frac{\partial T}{\partial Y}=0,\ K=0,\ \varepsilon=2\left(\frac{\partial\sqrt{K}}{\partial Y}\right)^2\quad 0\le X\le L$$

Numerical procedure: After a suitable non dimensionalization of the Eq. (1-6) and their boundary conditions (16), the finite volumes method was used for the discretization of this set of coupled non-linear differential equations.

The time scheme is semi-implicit and second order. It consists in the combination of the second order implicit Euler back ward scheme for the time term as follows:

$$\frac{\partial\phi^{\tau+\Delta\tau}}{\partial t}\approx\frac{3\phi^{\tau+\Delta\tau}-4\phi^{\tau}+\phi^{\tau-\Delta\tau}}{2\Delta\tau} \quad (17)$$

The explicit Adams-Bashforth scheme is used for the nonlinear terms following the relation:

$$(U.\nabla)\phi\big|^{\tau+\Delta\tau}\approx 2(U.\nabla)\phi\big|^{\tau}-(U.\nabla)\phi\big|^{\tau-\Delta\tau} \quad (18)$$

Implicit formula is used for the discretization of the viscous diffusion terms and the pressure gradients terms. For the space discretization, we have used the central difference scheme, having a second order accuracy for the momentum and the energy equations.

For the equation of turbulent kinetic energy and its function of dissipation, the hybrid scheme is employed. The hybrid scheme is largely employed for turbulence in square cavities to enhance numerical stability (Kuyper, 1993; Henkes and Hoogendoorn, 1994). In order to obtain numerical results we made our own computer code in FORTRAN, which contains some routines for preparing, initializing and solving. For the velocity-pressure coupling, the SIMPLER algorithm (Semi-Implict Method for Presses-Linked Equations Revised) was used. The sweeping method line by line, with the algorithm of Thomas was used for the iterative resolution of the systems of equations (Patankar, 1980).

The computations of high Rayleigh number flows, requires a fine numerical grid in regions adjacent to solid walls. To ensure that the calculated results are grid independent, 2 different non uniform square meshes have been employed, characterized, respectively by 70 and 80 nodes in each direction. The mesh is finer near the walls where we expect an important change of the physicals variables. The relative error between the 2 grids was about 7% for average Nusselt number, lower than 6% for the maximum normalized turbulent viscosity and lower than 1% for the maximum normalized vertical velocity.

To reach convergence the normalized sum of the absolute residuals for the discretized for the discretized equations should be less than $5*10^{-5}$ and the maximum normalized iterative change of all variables should be less than 10^{-5}.

RESULTS AND DISCUSSION

The control parameter of this study is the Rayleigh number based on the cavity section and the difference temperature between the hot and the cold wall:

$$Ra = \frac{g\beta(T_h - T_c)L^3}{\alpha\nu} \qquad 19$$

Two Rayleigh numbers have been used: $Ra = 1.58*10^9$ and $Ra = 4.9*10^{10}$, correspond respectively to the experiment of Tian and Karayiannis (2004) and to the numerical study of Sharif and Liu (2003). The Prandtl number for air is fixed at Pr = 0.71. For the two selected cases, the computations are started at $\tau = 0$ with a dimensionless time step of 10^{-5} and steady state solutions are obtained for both Rayleigh numbers.

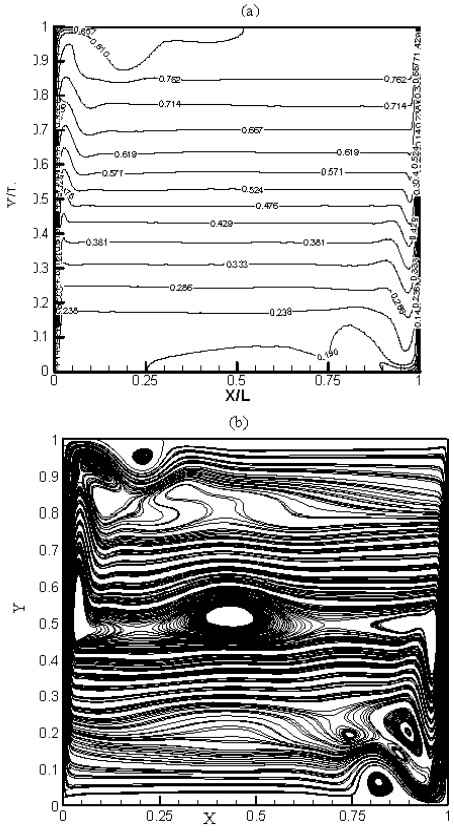

Fig. 2: Temperature contours (a) and streamlines (b) for $Ra = 1.58*10^9$

The case with $Ra=1.58*10^9$: This case was selected to be in direct comparison with the experimental results of Y.S. Tian and T.G. Karayiannis. The obtained numerical results are represented in the Fig. 2-5.

Figure 2 (a) shows the normalized temperature contours in the cavity considered. We note a stable thermal stratification according to the vertical direction, and a very weak variation (almost null) according to the horizontal direction, except for the adjacent zones close to the heated and cold walls, where thermal boundary layers are developed and where the temperature gradient is large.

By examining Fig. 2b which represents the streamlines of the flow considered, we noted the presence of a clockwise recirculation zone covering the entire cavity, in the inside of this zone, we noted the presence of two small vortices close to the vertical walls, and another one located in the mid-height of the cavity. In addition, small cells are located in the upper left corner and the bottom right corner of the cavity. All vortices are rotating not result from instability of the base flow but are a direct consequence of the convective distortion of the temperature field. The development of thermal boundary layers intensifies the vertical temperature gradient in the

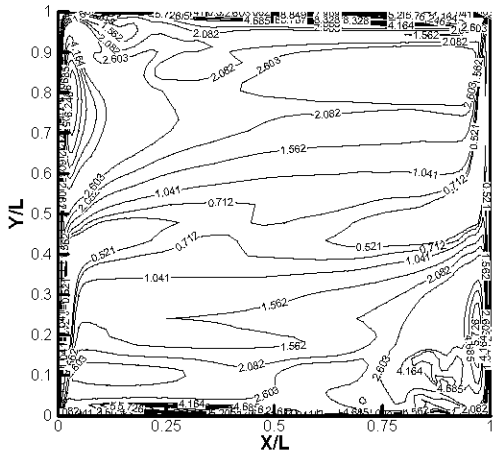

Fig. 3: Normalized turbulent viscosity distribution for Ra=1.58*10^9

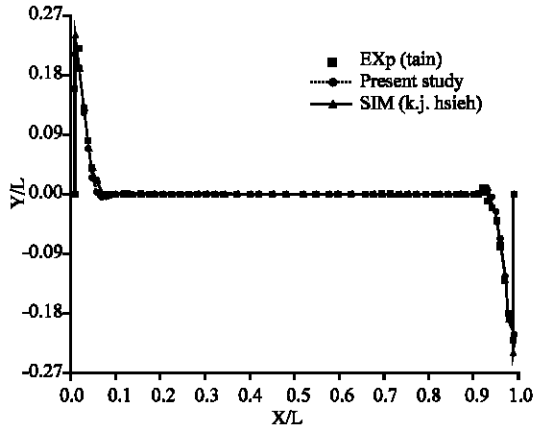

Fig. 4: Normalized vertical velocity profile at Y/L=0.5

vicinity of the walls. A vorticity sink thus separates the regions of concentrated vorticity generation and two secondary vortices are formed.

The ratio of the eddy viscosity to the molecular kinematics viscosity defined as:

$$\nu_t^* = \frac{\nu_t}{\nu} \tag{20}$$

presents a relative measure of the diffusive potential of the turbulence in cavities. Figure 3 shows the distribution of this quantity inside the cavity. The larger values are located near the upper horizontal wall and adjacent to the lower one. Maximum turbulent viscosity is more than ten times higher than the molecular viscosity.

Direct comparison of the normalized vertical velocity profile at mid-height of the cavity is shown in Fig. 4. The buoyant velocity is used as a normalization parameter for all the velocities:

Table 1: Average nusselt numbers

	$\overline{Nu}$ hot wall	$\overline{Nu}$ cold wall
Tian (2000)	64.00	65.3
Hsieh (2003)	54.68	54.52
Present study	68.34	68.93

$$V_0 = \sqrt{g\beta(T_h - T_c)L} \tag{21}$$

The normalized vertical velocity profile at mid-height shows a fast increase close to the hot wall and an abrupt reduction of this one close to the cold wall. In the remainder of the cavity, velocity is uniform. A very good agreement is obtained between our numerical results and the experimental results of Tian and Karayiannis (2000) and the numerical results of Hsieh and Lien (2004).

RANS model works quite well in predicting the average flow and heat transfer effect, thus can be applied to obtain the average Nusselt number results. The local Nusselt number which characterizes the heat transfer of the active walls, is defined as:

$$Nu = -\frac{L}{T_h - T_c}\frac{\partial T}{\partial n} \tag{22}$$

where, n is the normal surface.

The average Nusselt number is defined as:

$$\overline{Nu} = -\frac{\int_0^H Nu.dy}{H} \tag{23}$$

where H represents the cavity height (H=L). The following table (Table 1), compares the values of the average Nusselt numbers raised from the literature (Tian and Karayiannis, 2000; Hsieh and Lien, 2004) with those of this study.

Our numerical results overestimated the $\overline{Nu}$ by approximately 6.25%, where the numerical study of Hsieh and Lien (2004), using 4 different model variants underpredicts the $\overline{Nu}$ by 17%, which consistent with Henkes's study for a flow over a heated vertical plate, in which Nusselt was also underpredicted by 18% when the Launder-Sharma model with the Yap term was used. Experimental data for natural turbulent convection in cavities is hard to obtain, because small amounts of heat loss have a large effect on the outcome. The relation of correlation often adopted for literature as valid for the natural turbulence problems in cavities with thermally active vertical walls over a wide range of Pr numbers and aspect ratios (A=H/L) is:

$$\overline{Nu} = C.Ra^{1/3} \tag{24}$$

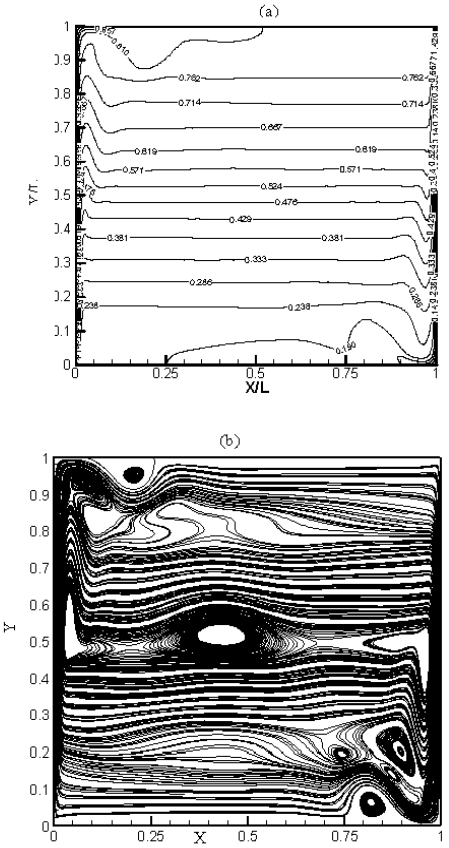

Fig. 5: Temperature contours (a) and streamlines (b) for Ra = $4.9*10^{10}$

where, C represents a coefficient which generally varies between 0.043 and 0.047 according to (Henkes and Hoogendoorns, 1994). For our case, the value: C=0.047 gives the best approaches.

The case with Ra = $4.9*10^{10}$: This case was selected to be in direct comparison with the experimental results extracted from Peng and Davidson (2001) and with the numerical results of Sharif and Liu (2003) using the k-ω turbulence model of Wilcox (1994) (KOM) and the k-ε turbulence model of Lam and Bremhorst (1993) (KEM).

The results found in this case, represent the same qualitative aspect as those found for the case with Ra = $1.58*10^{9}$. Air in the cavity rises along the hot wall and descends along the cold wall and turns at the corners, thus creating turbulent boundary layer along the 2 vertical walls and an almost stationary core. A higher Rayleigh number corresponds to a thinner boundary layer and a larger centre core, as can be seen from the temperature contours in Fig. 5 (a). Figure 5 (b), show streamlines of the flow. It seem that increasing Ra to $4.9*10^{10}$, causes the 2

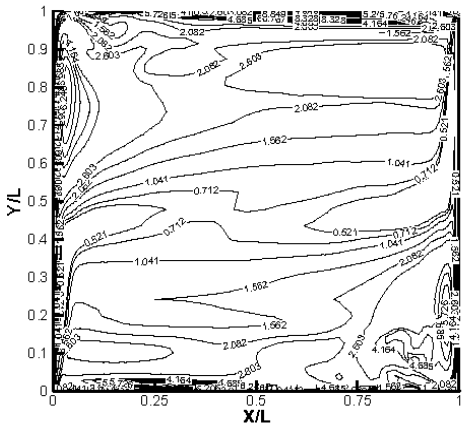

Fig. 6: Normalized turbulent viscosity distribution for Ra = $4.9*10^{10}$

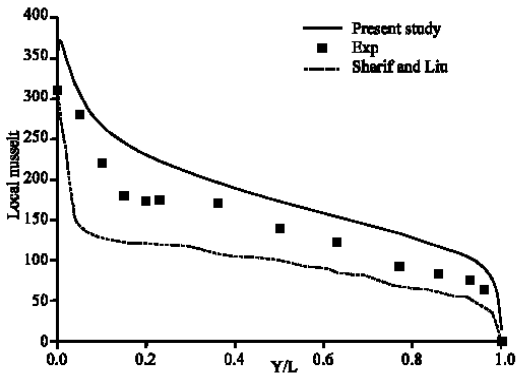

Fig. 7: Local Nusselt number profile along the hot vertical wall for Ra = $4.9*10^{10}$

secondary vortices to move closer towards the walls and are convected further downstream and the disappearing of the vortex in the central region.

Normalized turbulent viscosity is shown in Fig. 6. The higher values are located in the same locations as in the previous case. The maximum value is about 93.61, which is high compared to the maximum values obtained by others numerical studies, where low Reynolds number models are not used. These features illustrate best that reliable predictions could only be expected with turbulence models which incorporate adequate low Re number modifications as suggested by Hanjalic and Vasic (1993).

However, larger average Nusselt number was founded ($\overline{Nu}$ =181.54). This last value gives a relative error less than 5.5% when the relation of correlation (24) is adopted, where C=0.047. Comparison between local Nusselt number profiles along the hot vertical wall against experimental data and against Sharif's results is given in Fig. 7.

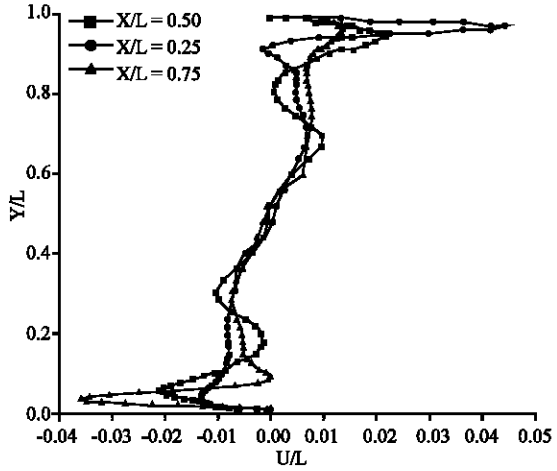

Fig. 8: Normalized U velocity profile for Ra = $4.9*10^{10}$

As can be seen, the largest values are obtained in the lower corner where the fluid cooled by the cold wall, comes into contact with the hot wall. A sharp decrease follows so that the Nu number falls practically to zero in the upper corner. Our numerical model overpredicted the local Nusselt number variation, while Sharif's model (KEM) underestimated the local Nusselt number. The transition to turbulence is indicated by a slight increase in Nusselt number at around Y/L=0.3- 0.4 in the experimental data. The KEM turbulence model and our model failed to predict this transition point.

The application of adiabatic conditions at the horizontal walls has been customary in studies of side-heated natural convection for long time. Such a configuration was expected to minimize the thermal influence of the horizontal walls on the flow.

Normalized horizontal velocity profile U/V_0 for various values of arbitrarily selected locations X/L is shown in Fig. 8.

It is clear that the highest velocities are located close to the hot wall near the higher corner and the lowest velocities are close to the cold wall near the lower corner. Inside the cavity and because of the stable thermal stratification, the velocities values are at least comparable in the various selected positions.

CONCLUSION

In this study, the LRN turbulence model of Launder (1974) is used for the resolution of the turbulent natural convection problem in a square cavity. The finite volumes method is employed for the discretization of the controlling equations. Algorithm SIMPLER is used for the pressure-velocity coupling and the sweeping method line by line with the algorithm TDMA is used for the iterative resolution of the systems of discretized equations. The global second order accuracy of the numerical method in space and in time proves the positive influence to the obtained results.

For Ra =$1.58*10^9$, our numerical results show an acceptable agreement with both the experimental results of Tian and Karayiannis (2000) and with the numerical results of Hsieh and Lien (2004) concerning the flow field and the turbulent viscosity, however an over estimation of about 6.25% is obtained for the average Nusselt numbers.

For Ra = $4.9*10^{10}$, the same behaviours like in the previous case were founded, with an increase in the average Nusselt number due to the increase in the Rayleigh number. Thermal and dynamic boundary layers are thinner than the previous case. However in this case, our numerical model failed to obtain the transition point from laminar to turbulent.

REFERENCES

Bett, P.L. and I.H. Bokhari, 2000. Experiments on turbulent natural convection in an enclosed tall cavity. Int. J. Heat Fluid Flow, 21: 675-683.

Cheesewright, R., J.R. King, S. Ziai, 1986. Experimental data for the validation of computer codes for the prediction of 2-dimensional buoyant cavity flows. In: ASME Winter Annual Meeting, Hemisphere HTD, 60: 75-81.

Davidson, L., 1990. Second-Order Corrections of the k-ε Model to Account for Non-Isotropic Effects Due to Buoyancy. Int. J. Heat Mass Transfer., 12 (33): 2599-2608.

Dol, H.S. and K. Hanjalic, 2001. Computational study of turbulent natural convection in a side-heated near-cubic enclosure at a high rayleigh number. Int. J. Heat Mass Trans., 44: 2323-2344.

Hsieh, K.J. and F.S. Lien, 2004. Numerical modelling of buoyancy-driven turbulent flows in enclosures. Int. J. Heat Fluid Flow, 25: 659-670.

Henkes, R.A.W.M. and C.J. Hoogendoorn, 1995. Comparison exercise for computational turbulence natural convection in enclosures. Numerical Heat Trans. B., 28: 59-78.

Hanjalic, K. and S. Vasic, 1993. Computation of turbulent natural convection in rectangular enclosures with an algebraic flux model. Int. J. Heat Mass Trans., 14 (36): 3603-3624.

Henkes, R.A.W.M. and C.J. Hoogendoorn, 1994. Scaling of the turbulent natural convection in a heated square cavity. J. Heat Trans., 116: 400-408.

Ince, N.Z. and B.E. Launder, 1989. On the computation of buoyancy-driven turbulent flows in rectangular enclosures. Int. J. Heat Fluid Flow, 2 (10): 110-117.

Kuyper, R.A., Van Der Meer, H. Th, C.J. Hoogendoorn and R.A.W.M. Henkes, 1993. Numerical study of laminar and turbulent convection in an inclined square cavity. Int. J. Heat Mass Trans., 11 (33): 2899-2911.

Launder, B.E. and D.B. Spalding, 1974. The numerical computations of turbulent flows. Comput. Meth. Applied Mech. Eng., 3: 269-289.

Lam, C.K.G. and K. Bremhorst, 1981. A Modified form of the K-ϵ model for predicting wall turbulence. Journal of Fluids.

Markatos, N.C., M.R. Malin and G. Cox, 1982. Mathematical Modelling of Buoyancy Induced Smoke Flow in Enclosures. Int. J. Heat Mass Trans., 25: 63-75.

Patankar, S.V., 1980. Numerical heat transfer and fluid flow. Mac Graw Hill, New York.

Sharif, M.A.R. and W. Liu, 2003. Numerical study of turbulent natural convection in a side-heated square cavity at various angles of inclination. Numer. Heat Trans. A., 43: 693-716.

Tian,Y.S. and T.G. Karayiannis, 2000. Low turbulence natural convection in an air filled square cavity. Part I: The thermal and fluid flow fields. Int. J. Heat Mass Trans., 43: 849-866.

Tanaka, H., S. Maruyama and S. Hatano, 1987. Combined forced and natural convection heat Trans for upwind flow in a uniformly heated vertical pipe. Int. J. Heat Mass Trans., 1 (30): 165-174.

Tanaka., Henkes, R.A.W.M. and C.J. Hoogendoorn, 1989. Comparison of turbulent models for the natural convection boundary layer along a heated vertical plate. Int. J. Heat Mass Trans., 1 (32): 157-169.

Yap, C.R., 1987. Turbulent heat and moment transfer in recirculating and impinging flows. Ph.D. Thesis, University of Manchester, Institute of Science and Technology.

Wilcox, D.C., 1994. Simulation of transition with a 2-equation turbulence model. AIAA J., 32: 247-254. Eng., 103: 456-460.